Energy & Buildings 359 (2026) 117312

Contents lists available at ScienceDirect

Energy & Buildings

journal homepage: www.elsevier.com/locate/enb

Non-Fourier heat transfer modeling for human skin under dynamic solar radiation: A dual phase-lag approach for outdoor thermal comfort assessment

Yuchen Ji [a], Wei Gu [b], Da Tao [a], Pengyuan Shen [c,*]

[a] College of Mechatronics and Control Engineering, Shenzhen University, Shenzhen 518052, China
[b] School of Architecture, Harbin Institute of Technology (Shenzhen), Shenzhen 518055, China
[c] Institute of Future Human Habitats, Shenzhen International Graduate School, Tsinghua University, Shenzhen, China

ARTICLE INFO

Keywords:
Dual phase-lag model
Non-Fourier heat transfer
Solar radiation
Outdoor thermal comfort
Thermophysiological modeling

ABSTRACT

Outdoor thermal comfort plays an important role in human health and daily activities, and is strongly affected by solar radiation, a primary source of heat stress in daily life. However, conventional Fourier-based models may oversimplify skin heat transfer, and neglect tissue inhomogeneity and temporal lag effects, especially under dynamic solar exposures. In this study, we developed a thermophysiological model based on dual phase-lag (DPL) theory to capture skin heat transfer under dynamic solar exposures. The model was solved using finite difference methods and validated against experimental data from 15 healthy participants exposed to intermittent solar radiation cycles. Results showed that the DPL-based thermophysiological model outperformed the conventional Pennes model, achieving 30% lower predictive errors (RMSE = 0.28 vs 0.40). While both models reproduced similar rising and falling patterns of skin temperature, the DPL approach better accounted for temporal lag effects, leading to more accurate predictions of thermal sensation. Moreover, analysis revealed that inner skin layers remained thermally stable under lower radiation levels, while the thermal stability became disrupted when radiation intensity exceeded 800 W/m^2. The influences of solar radiation duration and intensity on surface and inner skin temperatures were also systematically evaluated. Overall, the findings demonstrate that the proposed thermophysiological model could enhance the accuracy of thermal response prediction under dynamic solar radiation conditions and provide a strong basis for outdoor thermal comfort assessment and environmental design.

Nomenclature

Symbol	Description	Unit
c_{bl}	specific heat capacity of blood	J/(kg·K)
c	specific heat capacity of tissue	J/(kg·K)
k	thermal conductivity of tissue	W/(m·K)
Q_{bl}	heat exchange due to blood perfusion	W/m^3
Q_m	tissue metabolic rate	W/m^3
Q_r	radiative heat exchange rate	W
r	radial distance	m
T	tissue temperature	K
t	time	s
T_a	ambient temperature	K
T_{bl}	arterial blood temperature	K
T_{sk}	skin temperature	K
v_{bl}	local skin blood flow rate	1/s
w_{bl}	blood perfusion rate	1/s
ρ	tissue density	kg/m^3
ρ_{bl}	blood density	kg/m^3
α_{sk}	local tissue perfusion coefficient	
τ_q	relaxation time for heat flux establishment	s
τ_T	relaxation time for temperature gradient formation	s
Acronyms		
DPL	dual phase-lag model	
DTS	dynamic thermal sensation model	
LWR	long-wave radiation	W/m^2
PMV	predicted mean vote	
PPD	predicted percentage of the dissatisfied	
RMSE	root mean square error	
SWR	short-wave radiation	W/m^2

(continued on next column)

* Corresponding author at: Institute of Future Human Habitat, Shenzhen International Graduate School, Tsinghua University, Shenzhen 518055, China.
E-mail address: Pengyuan_pub@163.com (P. Shen).

https://doi.org/10.1016/j.enbuild.2026.117312
Received 26 October 2025; Received in revised form 14 January 2026; Accepted 11 March 2026
Available online 12 March 2026

1. Introduction

As ongoing climate change and urbanization affects the urban built environment [1,2], engaging in outdoor activities plays a crucial role in maintaining both physical and mental health. Thermal comfort is a key factor influencing individuals' choices regarding outdoor environments [3–5]. Among various environmental factors, solar radiation present a strong influence on human thermal comfort [6]. Solar radiation is a primary driver of hot outdoor conditions and directly impacts thermal physiological responses [7,8] and thermal perceptions [9]. While moderate solar radiation can be beneficial, such as UVB-induced vitamin D synthesis, excessive exposure poses serious health risks, and even lead to skin cancer [10]. In addition to ultraviolet damage, visible and infrared radiation can also cause skin injuries like sunburn [11]. As irradiation intensity increases, the permissible exposure duration decreases markedly. Beyond physiological risks, excessive solar radiation can lead to both thermophysiological strain and psychological discomfort [12]. Therefore, understanding the impact of solar radiation on human thermal comfort is of great importance.

In the outdoor environment, solar radiation varies considerably across seasonal, daily, and hourly timescales due to earth's orbital revolution around sun and its axial rotation. Seasonal variations are driven by Earth's orbital revolution around the Sun and its axial tilt, whereas daily and hourly variations result from Earth's axial rotation, which modulates the solar zenith angle [13]. In addition, individual exposure also fluctuates depending on activity type, behavioral patterns [14] and clothing properties (e.g., thermal insulation and color) [8] . From the psychological view, there could be time lag or advance between the human psychological response and the current environment in the dynamic environment. Physiologically, the heterogeneous structure of skin tissue leads to non-Fourier heat transfer behaviors, including temperature oscillations and fluctuations [15,16]. Both the environment and biological factors highlight the necessity of examining the effects of dynamic solar radiation on human thermal comfort from both psychological and physiological perspectives.

1.1. Thermophysiological mechanism of thermal comfort

Thermal sensation arises from nerve activity at thermoreceptors, which detect external thermal stimuli and transmit information to the brain, triggering perceptions of warmth or cold and activating thermoregulatory responses [17]. The heat transfer exchange between the human body and the thermal environment and nerve signal transmission forms the physiological mechanism of human body's thermal sensation, and thus thermal comfort is an inherently physiological and psychological construct [18–20].

Human thermophysiological model (such as Gagge's two-node model, Tanabe's model and Fiala's model) based on the heat balance equation and heat transfer theory are used to study the thermophysiological state of the human body [21–23]. When the environmental parameters are determined, the thermophysiological parameters (skin temperature, core temperature) of the human body can be determined by the thermophysiological models. Thus, the thermal comfort state can be determined by the thermophysiological parameters of the human body [14]. For example, in Gagge's two-node model, the thermophysiological model of the human body consists of passive and active systems. The passive system model is built based on body heat balance, including heat transfer between the environment and skin layer, and transfer between core layer and skin layer. Four active regulations, namely vasoconstriction, vasodilation, shivering and sweating, are considered, using the temperature difference between skin or core temperature and the reference temperature as the input signal to a linear regulation model [21]. When the air temperature changes abruptly, changes in the body's psychological responses, such as thermal sensations, will precede thermophysiological responses (skin temperature), especially when the temperature drops sharply. When the temperature rises suddenly, the physiological regulation of the human body is very rapid, the skin temperature rise is small, and the stabilization time is short, while the opposite is true when the temperature drops sharply [24]. For example, studies by Jacques B. Malchaire under fluctuating thermal conditions showed that rapid heating triggers prompt sweating responses that limit skin temperature rise and enable fast stabilization, whereas during rapid cooling sweating persists due to physiological delay, leading to larger skin temperature changes and longer stabilization times [25]. Zhang et al. verified the psychological advance phenomenon through experimental research, and established a binomial relationship between thermal sensation and skin temperature [26]. The phenomenon of physiological lag may be related to physiological regulation, and the weaker the physiological regulation, the more obvious the physiological lag. In addition, there are wave-like behavior and oscillations in the heat transfer process of the human body under dynamic radiation exposures, which deviates from the Fourier heat transfer theory [15,16]. Therefore, in the dynamic solar thermal comfort evaluation model, skin temperatures as a dynamic indicator of the model may cause a temporal bias for thermal comfort.

In thermal comfort evaluations, Predicted Mean Vote and Predicted Percentage of the Dissatisfied (PMV-PPD) is currently the most widely used steady-state predictive thermal comfort model [27]. However, PMV models are often biased in predicting thermal sensation in people's real-world environments, especially in naturally ventilated buildings and buildings where people can adjust themselves [28,29]. In addition, UTCI is a comprehensive strain index evaluating thermal comfort state [23], intended for steady or slowly varying outdoor conditions [30], limiting its applicability for evaluating dynamic outdoor thermal comfort. In a dynamic environment, human physiological and psychological responses lag or advance in time from the current environment, and thermal sensation and thermal comfort evaluation are not stable in a dynamic environment [31]. Currently, existing dynamic evaluation models primarily focus on thermal perception assessment related to changes in air temperature, such as the DTS model [32] and the R model [33]. However, the predictions of the modified TSV models were similar to those of the PMV model, whereas the DTS model exhibited significant discrepancies. Therefore, for dynamic thermal environments, especially dynamic solar radiation environments, traditional thermal sensation prediction models cannot derive additional thermal sensation changes due to dynamic temporal changes.

1.2. Thermal response of skin under solar radiation exposure

Various factors can affect thermal comfort and perception in the outdoor environment [34]. Among them, solar radiation is an influential factor considering its effect on human body heat balance [35], and its impact varies across regions and weather conditions, as evidenced in outdoor field studies [36]. Even in the same region, the solar radiation load can vary due to clothing factors, the position or activity [37–39]. Blazejczyk et al. found a strong correlation between physiological parameters and solar radiation as well as air temperature [8]. For standing people with 1 clo thermal insulation, approximately 68% of the variation in skin temperature can be explained by the combination of air temperature and solar radiation. 55% of the contribution can be attributed entirely to solar radiation. However, there exist discrepancies between predictions from thermophysiological models and experimental data [40–42].

In the context of outdoor thermal comfort, short-wave radiation (SWR) and long-wave radiation (LWR) exert distinct influences on the human body. LWR remains stable and primarily contributes as a constant background heat load [43]. In contrast, SWR exhibits pronounced temporal and spatial variability, governed by meteorological conditions, surrounding surfaces, and solar elevation, which together determine the fraction of radiation absorbed by the human body and strongly influence skin temperature responses. Infrared components of SWR further elevate skin temperature, and once thresholds exceeding 39 °C are reached, thermal strain is markedly intensified [44]. By comparison, the influence of LWR on thermal comfort is limited. Collectively, these findings indicate that SWR constitutes the dominant driver of both thermal and biological responses, whereas LWR exerts only a secondary, steady effect.

Considering the atmosphere, solar radiation reaches the human body through both direct and diffuse components. Direct radiation delivers concentrated energy from the sun, producing intense localized heating and glare when exposure is unobstructed. By contrast, diffuse radiation is scattered by molecules, aerosols, and clouds, arriving uniformly from the sky dome. as well as by diffuse reflection from the ground surface (ground scattering). Although less intense, diffuse radiation is persistent, even under shading or cloudy conditions, and therefore contributes to a continuous background load [45,46]. For human thermal comfort, direct radiation largely determines peak heat stress, while diffuse radiation sustains overall thermal exposure [47]. Since it is difficult to get the data of direct, diffuse and reflected solar radiation separately, solar radiation was simplified in the thermophysiological models, for example, in Fiala's model [23], radiation heat transfer was separated as SWR and LWR.

1.3. Thermophysiological model for skin temperature simulation

Mathematical thermobiological model can describe and predict body temperature distribution with environmental inputs. The most widely used model method is to apply the basic physical laws such as mass conservation, momentum conservation and energy conservation to any microelement of biological organism according to the continuum assumption and derive the biological heat and mass transfer equation by combining the constitutive equation reflecting various mass and energy transfer laws. These equations are usually expressed as a set of partial differential equations [48–55], which can be used to calculate the temperature distribution in the decomposition under certain initial and boundary conditions. However, we cannot fully understand all the relevant physical properties of various parts of the body, and the quantitative study of metabolic heat cannot meet the requirements of practical application. Therefore, simplified models are used in the actual research, such as the Pennes model [56], which assumes that the venous blood in the capillary seepage area is equal to the local body temperature, the Weinbaum anisotropic medium model, which classifies the blood flow effect into heat conduction, and the porous body model, which regards human tissues as porous media.

In typical thermophysiological models, such as the Gagge two-node model and the Tanabe multi-node model, the radiation heat exchange between the human body and the environment is only a function of the skin temperature and air temperature, and the solar radiation intensity is not directly added to the human body thermal balance model. Studies have shown that when considering the impact of direct solar radiation on human thermal comfort, it should be considered as a separate radiation component [57–59]. Therefore, in the Fiala-UTCI model and UC Berkeley physiological model, radiation heat exchange is regarded as an independent component in the heat balance equation. In addition, Gennusa et al. subdivided solar radiation into direct irradiation, diffuse and ambient radiation heat exchange, and correct the mean radiation temperature to explain the impact of solar radiation on human physiology [57]. Similarly, Blazejczyk et al. proposed a skin temperature assessment approach incorporating mean radiant temperature based on both SWR and LWR [60].

The above thermal physiological models are all based on the Pennes physiological model of the Fourier principle[21–23,61]. The Pennes equation distinguishes the heat transfer of biological tissues from that of general engineering materials for the first time, in the form of Equation (1). The model can reflect the heat transfer law of organisms, and only two parameters related to blood, namely, volume blood perfusion rate and local arterial blood temperature, are used to describe the results. Pennes model is based on the Fourier's law with an assumption of infinite speed of thermal energy transfer. In fact heat propagates with a finite speed in each medium like skin tissue with a non-homogeneous inner structure where the Pennes model fails to describe heat transfer process [62].

$$\rho c \frac{\partial T}{\partial t} = \Delta(k\Delta T) + Q_{bl} + Q_m + Q_{ext} \tag{1}$$

in which, ρ represents the density of biological tissue (kg/m^3), c is the specific heat capacity of the tissue (J/(kg·K)), T denotes the temperature of the biological tissue (K), t is time (s), k is the thermal conductivity of the tissue (W/(m·K)), Q_{bl} is the heat exchange due to blood perfusion (W/m^3), Q_m is the metabolic heat generation rate of the tissue (W/m^3), and Q_{ext} is external heat source (W/m^3).

In the outdoor environment, the solar radiation exposure to the human body is dynamic, and due to the non-uniform internal structure of biological tissues, as shown in Fig. 1. The epidermis is the outermost layer of the skin (thickness is about 0.4~0.2mm), and from the outside to the inside are the stratum corneum, the transparent layer, the granular layer, the spinous layer and the basal layer [63]. Below the epidermis is the dermis, which contains abundant accessory organs, blood vessels, nerves, etc. Due to the inhomogeneity of skin tissue, its heat transfer process exhibits non-Fourier behavior, and temperature oscillations and fluctuations in biological tissues have been observed in experiments [15 64]. Compared with the Fourier heat transfer model, the non-Fourier heat transfer model can better describe its thermal behavior [65,66]. Talukdar et al. employed a non-Fourier heat transfer model (specifically, the Dual Phase Lag (DPL) model) to analyze heat transfer in human skin under exposure to flame and radiant heat, emphasizing its accuracy in predicting thermal responses under short-term, high-intensity heat exposure [67]. In DPL models, two relaxation times are introduced to capture non-Fourier effects. Specifically, τ_q denotes the phase lag time for heat flux, which in biological tissues is interpreted as the interfacial resistance to heat transfer between different tissue constituents. Similarly, the time delay τ_T represents the characteristic time required for thermal activation at the microscale, arising from microstructural interactions within the tissue matrix [65]. The wave-dominated behavior ($\tau_q/\tau_T > 1$) observed with these parameter values is particularly relevant for skin tissue, where the heterogeneous structure creates preferential heat conduction pathways that lead to finite-speed thermal wave propagation rather than instantaneous diffusion-based heat transfer. Rapid changes in surface heating create steep temperature gradients that cannot be instantaneously established throughout the tissue depth. The multi-layered skin structure, consisting of the stratum corneum, epidermis, and dermis, exhibits different thermal responses due to varying thermal properties and vascular densities. In addition to conductive heat transfer within tissue layers, internal heat transport is strongly influenced by blood perfusion and vascular heat exchange. Research has consistently emphasized that internal human heat transfer is governed by the coupled effects of tissue conduction, blood perfusion, and active thermoregulation, commonly represented through Pennes bioheat equations embedded in multi-node thermophysiological models [23]. Vascular heat transfer plays a dominant role in rapidly redistributing heat between the body core and skin surface, thereby introducing additional temporal delays and spatial heterogeneity in skin temperature responses under dynamic thermal exposures [68]. Therefore, , blood flow regulation introduces additional temporal delays as the circulatory system responds to thermal stimuli through vasodilation and vasoconstriction mechanisms [56,69].

It is noteworthy that the 2021 Nobel Prize in Physiology or Medicine recognizes the discovery of a thermal receptor - the capsaicin receptor (TPRV1), as illustrated in Fig. 1 [70]. This receptor is not only related to the pain pathway, but also a heat-sensitive receptor. The discovery of this receptor explains the mechanism of thermal pain and is a crucial modality of thermal pain sensation [71]. In general, the multilayered and non-uniform structure of human skin leads to non-Fourier heat transfer behavior, and the thermal receptor (TPRV1) may play a critical

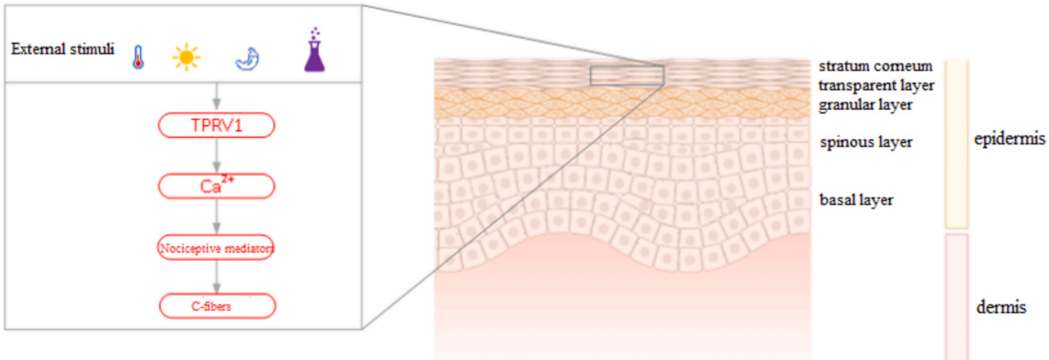

Fig. 1. Structure of skin layers and location of TPRV1 receptor.

role in thermal comfort under solar radiation exposure.

Therefore, to explore the mechanism of thermophysiological response under dynamic solar radiation exposure and describe the time lag effect of heat transfer in n non-homogeneous skin tissues, we proposed a heat transfer model based on a dual phase-lag model. To validate the model, we compared the simulated results with experiment data. In addition, the influences of solar radiation duration and intensity on the skin temperature of the inner and outer layers were explored. The research provides deeper insight into the transient thermal behavior of human skin, offering a valuable tool for both theoretical analysis and practical applications in health, safety, and environmental design.

2. Method

2.1. Dual Phase Lag (DPL) thermophysiological model development

2.1.1. Integration of DPL theory into thermophysiological framework

The conventional Pennes model assumes instantaneous heat propagation following Fourier's law, which may not adequately capture the thermal behavior of biological tissues under dynamic solar radiation exposure. Biological tissues exhibit non-Fourier behavior due to their heterogeneous structure, particularly in the skin where multiple layers with distinct thermal properties create complex heat transfer patterns. To address this limitation, we integrate the dual phase-lag (DPL) theory into the thermophysiological framework by replacing the traditional Fourier heat conduction formulation in the skin layer with the DPL constitutive equation.

The integration process involves modifying how heat flux within skin tissue is treated. Rather than employing the instantaneous relationship $q = -k\nabla T$, we utilize the DPL constitutive equation to account for finite relaxation times in both heat flux establishment and temperature gradient formation. The radiative heat exchange rate Q_r represents the net solar radiation absorption and becomes the critical component where non-Fourier behavior manifests under dynamic solar exposure conditions. While scattering alters the directionality of the radiation, it does not significantly shift its spectral composition. According to wavelength distribution, diffuse solar radiation is still classified as SWR, within the 0.3–3 μm range [72]. Besides, it is technically difficult in field comfort studies to partition global solar radiation into direct, diffuse solar radiation. Therefore, only the difference of heat transfer theory between SWR and LWR were considered in the study, and direct and diffuse solar radiation were not separated.

2.1.2. Dual Phase Lag constitutive equation

Due to the inhomogeneity of biological tissue, the heat transfer process cannot be fully explained by traditional Fourier theory. The DPL model, proposed by Tzou [65], accounts for the finite time required for heat flux (conductive heat transfer through heterogeneous tissue layers) establishment (τ_q) and temperature gradient development (τ_T):

$$q(r, t+\tau_q) = -k\nabla T(r, t+\tau_T) \quad (2)$$

In this formulation, τ_q represents the relaxation time for heat flux establishment, also known as the phase lag of heat flux, while τ_T represents the relaxation time for temperature gradient formation, referred to as the phase lag of temperature gradient. These parameters capture the finite speed of thermal signal propagation in heterogeneous biological tissues, which become particularly significant during rapid thermal transients such as those encountered during dynamic solar radiation exposure.

2.1.3. Mathematical development of the DPL-based governing equation

The development of the complete thermophysiological model incorporating DPL effects follows a systematic derivation process. First, we expand Equation (2) using Taylor series for small time increments, yielding:

$$q(r,t) + \tau_q \frac{\partial q}{\partial t} = -k\left[\nabla T(r,t) + \tau_T \frac{\partial \nabla T}{\partial t}\right] \quad (2a)$$

The energy conservation principle for biological tissue provides the fundamental relationship:

$$\rho c \frac{\partial T}{\partial t} = -\nabla \cdot q + Q_{bl} + Q_m \quad (2b)$$

where Q_{bl} and Q_m represent blood perfusion and metabolic heat generation, respectively. Taking the divergence of Equation (2a) and substituting into (2b) results in:

$$\rho c \frac{\partial T}{\partial t} + \rho c \tau_q \frac{\partial^2 T}{\partial t^2} = k\nabla^2 T + k\tau_T \frac{\partial \nabla^2 T}{\partial t} + \rho_{bl} w_{bl} c_{bl}(T_{bl} - T) + Q_m + \tau_q \frac{\partial}{\partial t}(Q_{bl} + Q_m) \quad (2c)$$

where, ρ_{bl} is the blood density (kg/m^3), w_{bl} is the blood perfusion rate (1/s), c_{bl} is the specific heat capacity of blood (J/(kg·K)), T_{bl} is the arterial blood temperature (K).

For practical implementation, we introduce dimensionless variables and assume quasi-steady blood perfusion and metabolic terms, leading to the final governing equation as described in the next subsection.

2.1.4. Complete DPL-based thermophysiological equation

The dimensionless parameters are defined as follows: $\theta = \frac{T - T_0}{T_0}$ represents the dimensionless temperature, $x = \frac{r}{L}$ is the dimensionless spatial coordinate, $F_o = \frac{kt}{\rho c L^2}$ denotes the Fourier number, $F_{oq} = \frac{k\tau_q}{\rho c L^2}$ and $F_{oT} = \frac{k\tau_T}{\rho c L^2}$ represent the dimensionless heat flux and temperature gradient relaxation times, respectively. Additionally, $P_m = \frac{Q_{m0} L^2}{k T_0}$ represents dimensionless metabolic heat generation, and $P_f = \sqrt{\frac{w_{b0} c_b}{k}} L$ represents the dimensionless blood perfusion parameter, $f(\theta)$ represents blood perfusion rate coefficient [73]. The complete governing equation (4c) for skin temperature under DPL theory becomes:

$$F_{0q}\frac{\partial^2\theta}{\partial F_o{}^2}=\frac{\partial^2\theta}{\partial x^2}+P_f{}^2f(\theta)(\theta_b-\theta)+F_{0T}\frac{\partial^3\theta}{\partial F_o\partial x^2}+\left[F_{0q}P_f^2f'(\theta)-F_{0q}P_f^2f(\theta)-1\right]\frac{\partial\theta}{\partial F_o}+P_m \tag{3}$$

An important verification of our formulation is that when $F_{0q} = F_{0T} = 0$, Equation (3) can be reduced to the classical Pennes equation, confirming the consistency of our mathematical development.

The selection of DPL relaxation time parameters requires careful consideration of the physical characteristics of biological tissues under thermal loading. In this study, we employed $\tau_q = 28$ s and $\tau_T = 20$ s based on established literature values for skin tissue applications [74]. Kumar et al. validated that the two parameter ranges are appropriate for dual-phase lag bioheat transfer modeling in thermal therapy applications, where the ratio $\tau_q/\tau_T > 1$ indicates wave-like behavior dominates over diffusion-like behavior in the heat transfer process [74]. The selected parameter values ($\tau_q/\tau_T = 1.4$) fall within the wave-dominated regime, which is consistent with the non-Fourier behavior expected in heterogeneous biological tissues under dynamic solar radiation exposure. These values have been validated in similar bioheat transfer applications involving rapid thermal transients and provide a reasonable foundation for modeling skin thermal response under solar radiation conditions [74,75]. Under dynamic solar radiation conditions, these lag times become particularly significant.

2.1.5. Numerical implementation and finite difference scheme

The numerical solution of the DPL-based thermophysiological equation requires careful discretization due to the presence of mixed temporal-spatial derivatives. We employ a finite difference approach where the temporal and spatial derivatives are approximated using central difference schemes. The temporal derivatives are discretized as $\frac{\partial\theta}{\partial F_0} = \frac{\theta_{i,k+1}-\theta_{i,k}}{\tau}$ and $\frac{\partial^2\theta}{\partial F_0{}^2} = \frac{\theta_{i,k+1}-2\theta_{i,k}+\theta_{i,k-1}}{\tau^2}$, while the spatial derivative follows $\frac{\partial^2\theta}{\partial x^2} = \frac{\theta_{i+1,k}-2\theta_{i,k}+\theta_{i-1,k}}{h^2}$.

The mixed temporal-spatial derivative requires special attention and is approximated as:

$$\frac{\partial^3\theta}{\partial F_0\partial x^2}=\frac{1}{h^2}\left[\frac{\theta_{i+1,k}-\theta_{i+1,k-1}}{\tau}-2\frac{\theta_{i,k}-\theta_{i,k-1}}{\tau}+\frac{\theta_{i-1,k}-\theta_{i-1,k-1}}{\tau}\right] \tag{6}$$

where $\theta_{i,k}$ represents the dimensionless temperature at the i-th spatial node and k-th time step, τ denotes the time step, and h represents the spatial step. The stability criterion for this mixed-derivative system requires $F_o = \frac{k\tau}{\rho c h^2} < \frac{1}{2\left(1+\frac{F_{0q}}{\tau^2}\right)}$ to ensure numerical stability while accounting for the additional temporal derivative terms introduced by the DPL formulation [76].

2.1.6. Solution algorithm and implementation strategy

The solution procedure follows a systematic approach beginning with the initialization of the temperature distribution and boundary conditions. For each time step, the discretized equation system is solved iteratively, with convergence checks ensuring that temperature changes between iterations remain below the specified tolerance. Dynamic solar radiation boundary conditions are updated at each time step to reflect the varying environmental conditions, and post-processing converts the dimensionless results back to physical temperatures. This approach ensures the capture of both the surface temperature responses governed by both body–environment heat exchange and internal heat transfer, and the delayed inner layer response that characterizes non-Fourier heat transfer in biological tissues. The implementation accounts for the complex interplay between surface heating from solar radiation and the depth-dependent thermal response of the multilayered skin structure.

2.2. Experiment validation

A total of 15 healthy and neat participants were recruited in this study, including 7 males and 8 females. During the experiment, the subjects stood still, wearing uniform clothes to ensure equal thermal insulation, which was about 0.6 clo (wearing white, polyester fiber short sleeved T-shirt and light-colored, cotton thin trousers). Demographic information is shown in Table 1. In each experiment, two subjects participated except for the last group with only one participant, and eight groups of experiments were conducted around 10 a.m. and 2 p.m.

Considering the influence of solar radiation intensity and outdoor stay time on physiological parameters, the objective outdoor thermal environment parameters (solar radiation intensity, air temperature, relative humidity, wind speed) are recorded as shown in Fig. 3. The skin temperature of the forehead, back, abdomen, back of the hand and calf is measured. Instrument information is listed in Table 2. Intermittent solar radiation exposures were designed in the field experiment. A 5-min solar exposure followed by a 5-min shadow stay for three loops was set, as illustrated in Fig. 2.

2.3. Environmental conditions

2.3.1. Air temperature and relative humidity

The air temperature and relative humidity during the eight experimental tests are shown in Fig. 4, in which the numbers 1-8 represent the eight experiment groups. In groups (1) and (2), the air temperature ranged from 28.5 to 30.0 °C, while in groups 3 to 5 the air temperature range varied from 32.3 to 34.1 °C. The maximum temperature change in the five groups was 1.1 °C, and the standard deviations were 0.09, 0.43, 0.33, 0.28, and 0.34 °C, respectively. The variation range of relative humidity was between 52% and 61%. Although there were some fluctuations, the overall range of variation was relatively small.

2.3.2. Wind speed

Table 3 summarizes the wind speed of the eight experiment groups. The wind speed varies mainly in 0.34 to 1.81 m/s, without a rule in time scale. The distributions of wind speed in groups (1), 2, 7 and 8 are similar, and groups 4, 5, and groups (3), 6 have a similar distribution, respectively.

2.3.3. Global solar radiation intensity and long-wave radiation

Solar radiation is an important factor affecting human thermal comfort, and its variation range is an important factor affecting human thermal responses in this experiment. The variation values of total solar radiation in the five groups of experiments are shown in Fig. 5. The global solar radiation intensity of groups (1) and (2) is about 700 W/m^2, and the global solar radiation intensity of the third to fifth groups is about 800, 900, and 1000 W/m^2, respectively. Due to the shading of clouds, the global solar radiation intensity is relatively low in the solar exposure stage of the sun in some working conditions.

The absorbed solar radiation load on the human body was estimated using six-directional solar radiation measurements, which provide irradiance incident on six orthogonal planes. For a standing human subject, the body was approximated as an upright convex geometry, for which radiative exposure is dominated by vertically oriented surfaces. Following established outdoor radiation-balance formulations and ISO 7726 recommendations [78], greater weighting was assigned to lateral

Table 1
Demographic information.

	Age	Height(cm)	Weight(kg)	BMI(kg/m2)
Max	27	179	80	28.7
Min	19	158	45	17.3
Mean	23.9	167.5	58.1	20.68
Std. Dev.	1.69	5.91	10.01	3.33

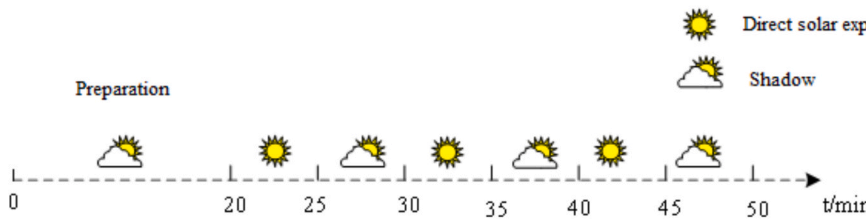

Fig. 2. Experiment procedure.

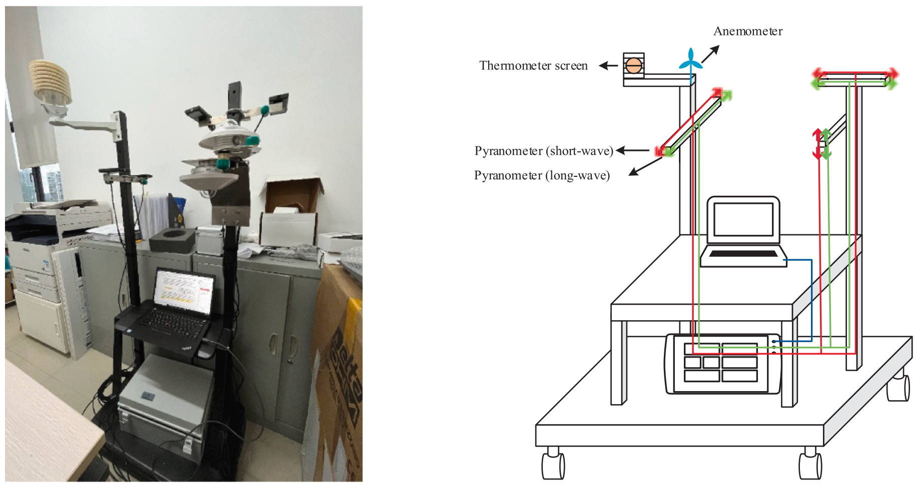

Fig. 3. Experiment instrument prototype and illustration.

Table 2
Instrument information.

	Type	Parameter	Precision	Range
Thermometer	HOBO U12-012	Air temperature	±0.35℃	-20~70℃
		RH	±2.5%	5% ~ 95%
Anemometer	TJHY WFWZY1	Wind speed	5% ± 0.05m/s	0.05~30m/s
Pyranometer	DELAOHM LPPYRA02S	Short-wave radiation	10μV/(W/m2)	0~2000W/m2
Pyranometer	Apogee SL-510-SS	Long-wave radiation	0.12mV/(W/m2)	-200 to 200W/ m2
Ibutton	i Button DS1923	Surface temperature	±0.5℃	-20~85℃

(vertical) irradiance components than to upward and downward components. The absorbed solar radiation load averaged over the body surface was calculated as Equation (7).

$$R_{sw,abs} = \alpha_{sw}\left(0.15 \times \left(R_{sw,down} + R_{sw,up}\right) + 0.175 \times \left(R_{sw,left} + R_{sw,right} + R_{sw,fore} + R_{sw,back}\right)\right) \quad (7)$$

where, $R_{sw,abs}$ is the absorbed solar radiation load (W/m^2), α_{sw} is short-wave absorptivity of clothing (set to 0.4 according light-colored clothing), $R_{sw,down}$, $R_{sw,up}$, $R_{sw,left}$, $R_{sw,right}$, $R_{sw,fore}$, $R_{sw,back}$ are solar radiation in six directions. The absorbed solar radiation was calculated in Fig. 6. The absorbed solar radiation under solar exposure was around 100-120 W/m^2, while under shade it was around 20-30 W/m^2.

Long-wave radiation is relatively stable compared with solar radiation, and there is no significant difference under direct solar radiation exposure and non-direct solar radiation exposure. Table 4 summarizes the mean value of long-wave radiation. Upward long-wave radiation is

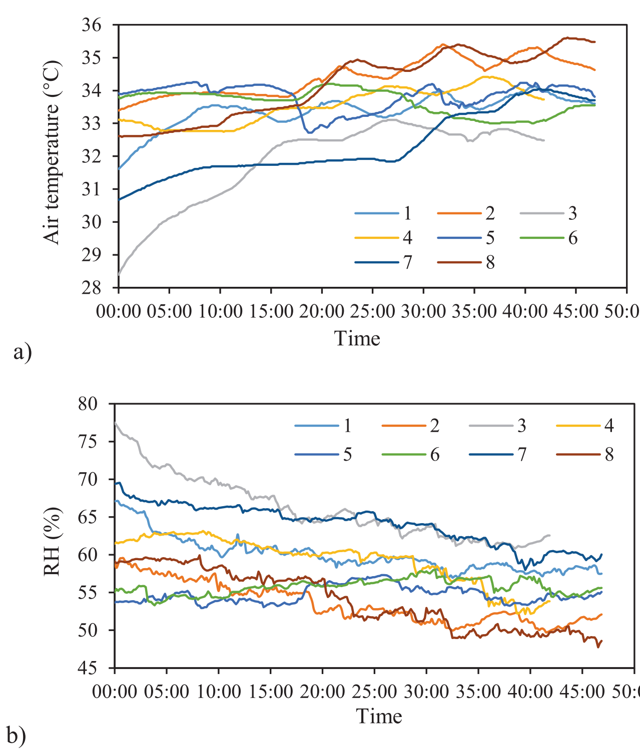

Fig. 4. Outdoor air temperature and relative humidity a) air temperature, b) relative humidity.

Table 3
Statistic summary of wind speed.

Group No.	Mean	Std. Dev.	Min	Upper quartile	Medium	Lower quartile	Max
1	0.99	0.65	0.11	0.45	0.85	1.38	3.18
2	1.02	0.66	0.11	0.46	0.91	1.42	3.41
3	0.69	0.41	0.11	0.37	0.62	0.90	2.11
4	1.33	0.84	0.14	0.66	1.24	1.81	5.48
5	1.33	0.65/	0.13	0.92	1.32	1.70	4.68
6	0.67	0.41	0.09	0.34	0.60	0.92	2.05
7	0.98	0.63	0.12	0.46	0.90	1.37	3.44
8	0.99	0.65	0.11	0.45	0.85	1.38	3.18

obviously larger than downward long-wave radiation. The horizontal long-wave radiation is similar.

3. Results and analysis

In this work, the temperature distribution in living skin tissue obtained from non-linear DPL model of bio-heat transfer is studied when outer surface is subjected to a sinusoidal heat flux. We have taken the temperature dependent blood perfusion such as a constant, linear and exponential variation and constant metabolic heat source in non-linear DPL bioheat transfer model. Only the parameters whose values differ from reference value are indicated. The selected reference value of dimensional parameters to compute the dimensionless temperature distribution in living skin tissue in finite domain are as follows: ρ=1000 kg m^{-3}, c = 4×103 Jkg^{-1}K^{-1}, k = 0.5 Wm^{-1}K^{-1}, Q_m = 33800 Wm^{-3}, T_b = 37℃, c_b = 3500 Jkg^{-1} K^{-1}, w_b = 8 kg m^{-3}s^{-1}, τ_q = 28 s, τ_T = 20 s, a_1 = 1.15, a_2 = 1 and T_o = 34℃, L= 0.05 m, q_0 = 155 Wm^{-2}, ω = 7.5 × 10^{-3} s^{-1}.

For difference equations in display format, the setting of time step and spatial step needs to consider the stability of equation solving. Within the stability range of the solution, the larger the time step (τ), the smaller the computational workload and the faster the computation time. For one-dimensional problems, $1/4<F_o=\frac{kt}{\rho cL^2}<1/2$ was generally required. In our computational work, we have chosen grid spacing length = 0.0125 and time step length =0.001.

3.1. Model validation

The experiment data was used as boundary conditions for the model. The simulated skin temperatures were compared with measured skin temperatures as Fig. 4. Meanwhile, to compare performance of DPL model with the original Pennes model, the simulated skin temperatures of Pennes model are also shown in the Fig. 7. As the results show, the skin temperatures simulated with DPL model are commonly closer to the experiment data.

Comparing the simulated results of the DPL model and the Pennes model, it can be found that during the process of skin temperature rise, the skin temperatures of DPL model show a slower change rate in a smoother curve and are more consistent with the experimental results. On the other hand, the results of Pennes model change fast with a steeper rise curve in the early stage and a smoother rise curve in the later stage. During the process of skin temperature decrease, the DPL model decreases more solely compared to the Pennes model. The above change law indicates that the skin temperature caused by exposure to solar radiation does not fully follow Fourier's law of heat transfer and needs to be corrected by a time lag factor.

In order to compare the accuracy of the DPL model and the Pennes model, Fig. 8 shows the root mean square error (RMSE) between the results of two models and the experimental results. The results showed that the DPL thermophysiological model has a better performance with a smaller RMSE than the Pennes model. However, the RMSE results also indicate that there are significant differences in accuracy under certain

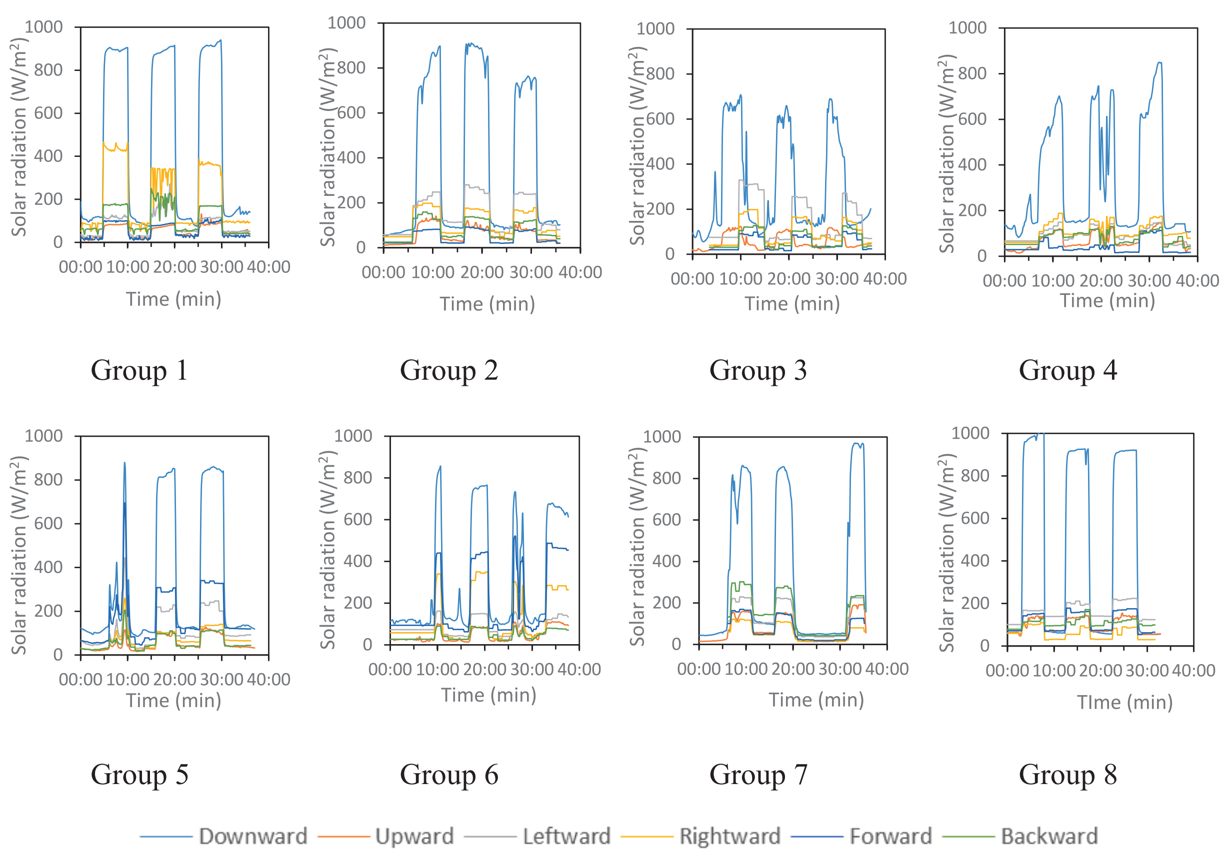

Fig. 5. Variations of global solar radiation.

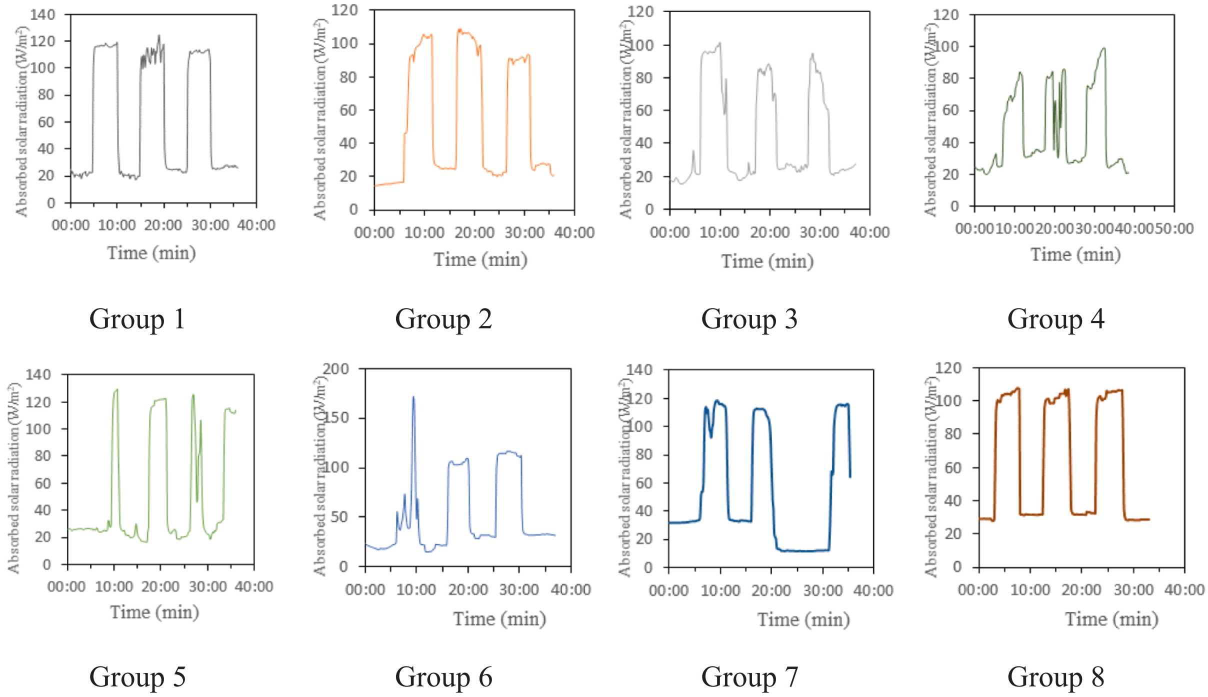

Fig. 6. Variations of absorbed solar radiation

Table 4
Mean value of long-wave radiation (Unit: W/m^2)

Group No.	Downward	Upward	Leftward	Rightward	Forward	Backward
1	427.66	517.48	496.28	502.58	490.14	496.36
2	421.46	517.50	496.10	502.52	489.95	496.16
3	422.47	518.51	496.05	503.29	489.50	496.11
4	419.50	521.01	496.00	502.74	489.45	496.06
5	419.51	520.99	495.96	502.72	489.79	495.98
6	419.50	521.01	496.00	501.74	489.45	496.06
7	419.46	520.99	495.93	502.70	489.71	495.98
8	419.58	520.97	495.83	502.56	489.60	495.92

conditions, which may be attributed to environmental factors and individual differences. Overall, the calculation results of the DPL model are closer to the experiment results than those of the Pennes model.

To examine the numerical improvements, the measurement uncertainties were performed. The resolution of skin temperature meter (iButton DS1923) is 0.0625 °C. As each iButton was individually calibrated in a NIST- -Traceable Chamber, and calibration coefficients has already been programmed into nonvolatile (NV) memory [79], the calibration uncertainty was neglected. Consequently, the measurement uncertainty (0.0625 °C) was smaller than the model discrepancy, supporting the validity of the results to some extent.

3.2. *Influences of exposure time and intensity on thermophysiology*

To further quantify the effects of exposure time and solar radiation intensity on skin temperature evolution, the above mathematical model was employed to simulate the transient skin temperature distribution across skin depth, allowing detailed analysis of both spatial temperature gradients and temporal variations under different solar exposure scenarios.

3.2.1. *Exposure time*

As solar exposure time and intensity has strong impacts on human health and thermal comfort, we further explored the influences of the two factors on skin temperatures based the proposed DPL model. To analyze the impacts of solar exposure time on skin temperature fluctuations, we simulated the skin temperatures under three time-steps of 5 min, 10 min and 15 min, exposed to 800 W/m^2. Here we focus on the skin temperature variations with depth, so the skin temperature can refer to any body segment only if exposed to solar radiation directly. The simulated results were illustrated in Fig. 9.

As shown in Fig. 7, the similarity of human skin temperature changes at different time intervals is that the skin temperature changes faster when entering or leaving solar radiation exposure. The skin temperature can basically reach stability at 15-minute interval, and the peak skin temperature is slightly higher than the skin temperature at 5-minute interval, close to skin temperature peak at 10-minute interval. This means that the first few minutes of sun exposure have a great impact on human skin temperature. Although long-term sun exposure will not cause a large change in skin temperature, the cumulative effect of solar exposure will cause greater damage to the health of human skin.

Fig. 10 shows the change rate of human skin temperature at different time intervals. Under the solar radiation exposure at 15-minute interval, the change rate of skin temperature is finally close to 0 in each stage. The rise and drop patterns of skin temperature are consistent, and the absolute value of the change rate is generally the same. However, since the human body's cold and heat receptors are independent and the number of cold receptors is relatively large, people are more sensitive to cold than heat. Therefore, although the skin temperature change law is similar, the changes in cold and heat sensations will be different.

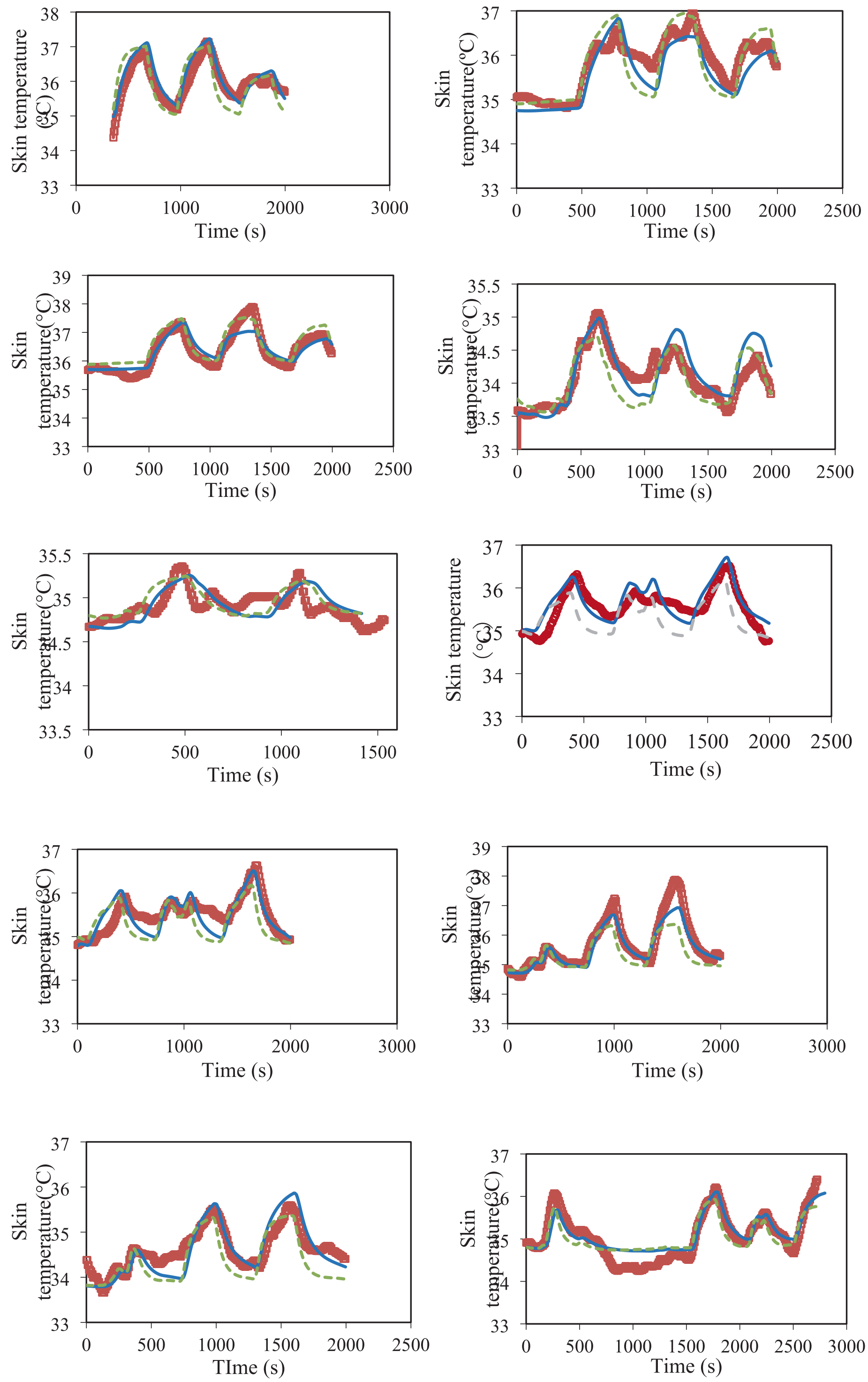

Fig. 7. Performance of dual-lag model compared with Pennes model and experiment.

Fig. 11 shows the temperature change of the inner skin layer at different time intervals. The results show that the peak temperature values of the inner skin layer are significantly different under the three intervals, and skin temperature does not reach stability at three intervals. For the solar radiation exposure at 5-minute interval, the temperature fluctuation of the inner layer of the skin is the smallest. At the three intervals, the temperature change of the inner layer is not obvious in the early stage of solar radiation exposure, and the skin temperature does not change significantly until 10 minutes later.

As shown in Fig. 12, by comparing the temperature of the surface and inner layers of the skin, it can be found that the temperature change of the surface layer is more obvious. In addition, there is a significant time lag in the temperature change of the inner layer. At the 15 min interval, the surface temperature and the inner layer temperature are generally opposite. The skin temperature changes alternately with the depth, but the surface temperature changes significantly and the inner skin temperature changes less, which has a more complex mechanism of affecting the thermal sensation.

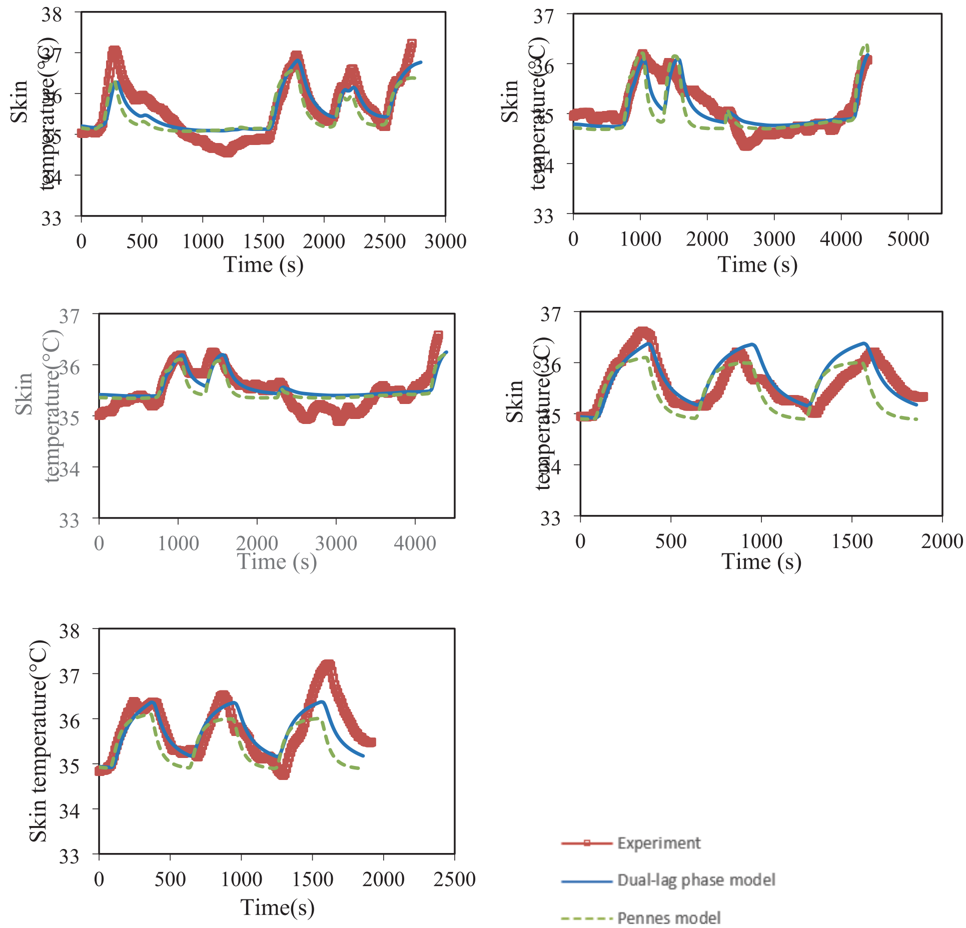

Fig. 7. (*continued*).

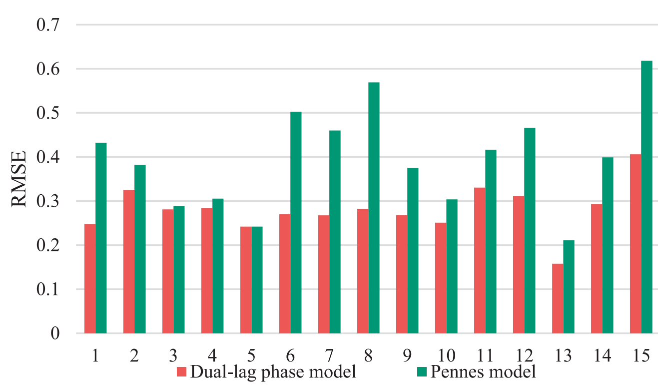

Fig. 8. RMSE of Dual phase lag model and Pennes model with experiment data.

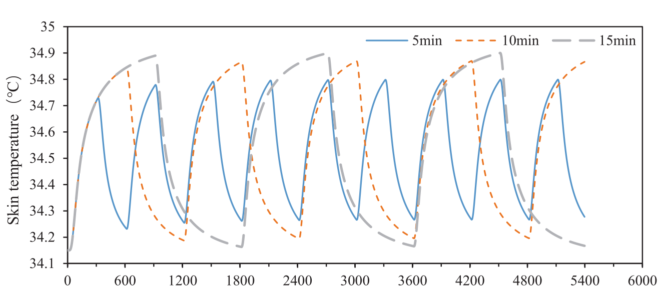

Fig. 9. Simulated skin temperature variations under different time-steps.

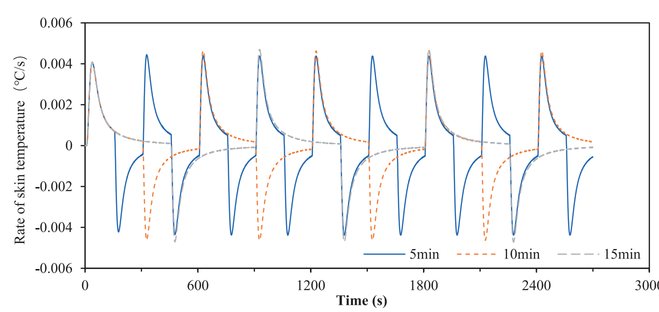

Fig. 10. Change rate of skin temperature under different time-steps.

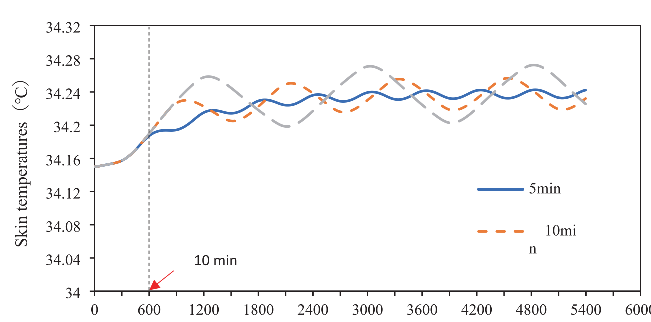

Fig. 11. Skin temperature at inner layer under different time steps.

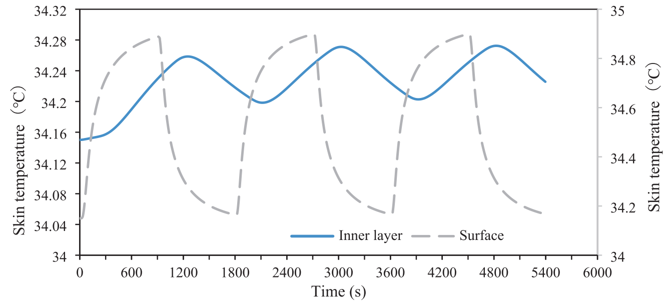

Fig. 12. Comparison of skin temperature at surface and inner layer at 15 min interval.

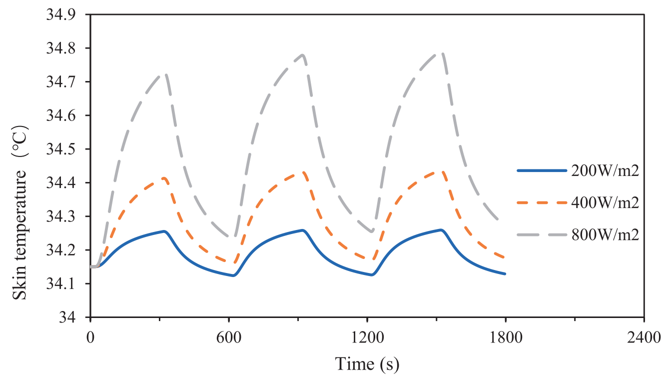

Fig. 13. Skin surface temperature under three solar radiation intensities.

3.2.2. *Solar radiation intensity*

In order to explore the changes in human skin temperature under different solar radiation intensities, we set three radiation intensity conditions of 200, 400, and 800 W/m^2. Fig. 13 illustrates the temperature changes in the skin surface. It can be seen that the change laws of the three radiation intensities are relatively similar, but the temperature amplitudes fluctuate due to different radiation intensities are different. The skin temperature change amplitudes are proportional to the solar radiation intensity according to the simulation results.

Fig. 14 shows the skin temperature change of the inner layer. In addition to the temperature delay phenomenon, it can be seen that the temperature of the inner layer can generally reach stability under the conditions of 200 W/m^2 and 400 W/m^2, while under the condition of 800 W/m^2, the temperature of the inner layer has been rising. Therefore, at a low radiation exposure level, the temperature stability of the inner skin layer is good, but when the radiation intensity exceeds a certain level, the stability of the skin temperature will be broken.

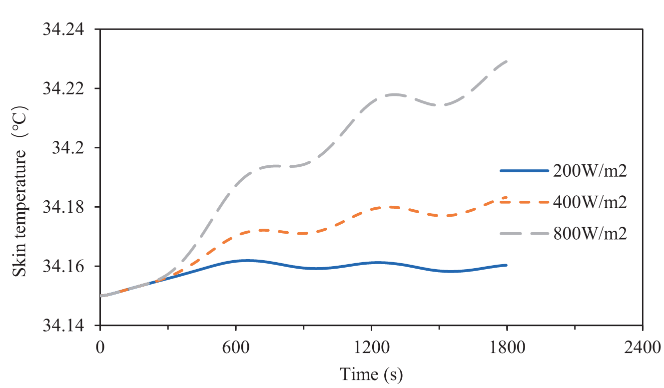

Fig. 14. Skin temperatures at inner layer under three intensities.

4. Discussions

4.1. *Physical mechanisms of lag effects in skin heat transfer*

As non-homogeneous inner structure such as biological tissues or high-power with short duration may break down Fourier's law, steep changes of solar radiation exposure (solar radiation intensity step-change between 50 W/m^2 and 1000 W/m^2) to skin tissues will induce temperature lag in skin heat transfer [77]. Besides, considering sunburn and actual solar exposure conditions, 5-min step change of solar radiation exposure was applied. DPL model was well applicable in periodic change of 2-5 min [75,80]. Therefore DPL model was introduced here to model the temperature distribution of the whole skin tissue.

The results demonstrate that skin temperature exhibits steep changes when entering solar exposure, with rapid temperature change rates at the onset of exposure. This phenomenon results from dynamic thermal properties of skin tissue that vary proportionally with exposure time. Previous studies have established that thermal properties such as heat capacity and thermal resistance increase with exposure duration [81], indicating that at exposure initiation, these properties are relatively small and skin temperature becomes more vulnerable to solar stimuli.

Solar stimuli induce cutaneous vasodilation and eccrine sweating [82,83] as thermoregulatory responses to maintain thermal homeostasis. These physiological adaptations create a dynamic thermal balance that evolves throughout the exposure period, explaining the transition from rapid initial temperature rise to eventual stabilization observed in our simulations. The pronounced delay in inner skin temperature relative to surface temperature reflects the fundamental architecture of human skin, where traditional thermoreceptors are located 0.3-0.6 mm below the surface in the dermis, while thermoreceptors sensitive to high-temperature stimulation (TRPV1) are predominantly located in the epidermis [71]. This spatial distribution creates temporal disconnect between surface heating and deep tissue thermal sensation [77].

4.2. *Model performance and validation*

The DPL thermophysiological model achieves superior predictive accuracy compared to the conventional Pennes model, with RMSE values of 0.28 and 0.40, respectively, representing a 30% reduction in prediction error. During temperature rise phases, the DPL model exhibits more gradual change rates with smoother curves that align closely with experimental observations, while the Pennes model demonstrates rapid changes characterized by steep initial rises followed by gradual increases. The temperature decrease phase reveals even more pronounced differences, with the DPL model producing more uniform decreases, indicating that thermal relaxation times better represent physical mechanisms governing heat dissipation in skin tissue. Thermal lag times τ_q and τ_t gives freedom to modify the Pennes model to better describe the skin temperature, which consider the procedures of temperature gradient and heat flux [65,80,84].

The superior performance aligns with previous validation studies where DPL-based bioheat models predicted burn onset times within ±10% of experimental observations, while Fourier-based predictions underestimated onset times by up to 25% [67]. Similar results have demonstrated that DPL models provide better prediction in skin temperature compared with Fourier-based models [85,86]. The improved accuracy stems from the DPL model's ability to account for finite relaxation times in both heat flux establishment and temperature gradient formation, enabling simulation of thermal wave behavior and delayed heat propagation under dynamic thermal loading conditions.

4.3. *Implications for thermal comfort and sensation*

The time lag phenomena have significant implications for understanding human thermal comfort under dynamic solar radiation. Although temperature rise and fall patterns exhibit similar magnitudes and shapes, human thermal perception differs substantially due to asymmetrical distribution of thermal receptors. The higher density of cold receptors makes individuals more sensitive to cooling than heating, suggesting thermal sensation models must account for this physiological asymmetry.

The 15-minute exposure intervals reveal that surface and inner skin temperatures often exhibit opposite trends, creating complex depth-dependent temperature alternation. Surface temperatures show pronounced fluctuations while inner layer temperatures demonstrate stable responses with significant temporal delays. This multi-layered thermal response cannot be captured through surface measurements alone and suggests thermal comfort assessment requires consideration of depth-dependent thermal gradients.

Analysis of different radiation intensities reveals important threshold effects. Under low radiation levels (200-400 W/m^2), the inner skin layer maintains good thermal stability, but when intensity exceeds approximately 800 W/m^2, inner layer temperature exhibits continuous rise without reaching stability, indicating breakdown of thermal homeostasis. This threshold behavior has important implications for thermal comfort guidelines and safety standards, suggesting a critical radiation intensity beyond which skin thermal regulatory mechanisms become insufficient.

The enhanced accuracy of the DPL-based model provides a reliable foundation for evaluating outdoor thermal comfort in architectural and urban planning applications. The model's ability to capture both immediate surface responses and delayed deep tissue effects makes it valuable for designing outdoor spaces, shade structures, and building facades that optimize thermal comfort while minimizing heat stress. The temporal aspects suggest that thermal comfort assessment protocols should consider exposure duration and intensity patterns rather than relying solely on instantaneous environmental measurements.

The model's capability to predict threshold effects and thermal stability breakdown has important applications in occupational health and safety. Industries involving outdoor work, sports, and recreational activities could benefit from improved exposure guidelines based on enhanced understanding of skin thermal responses. The model could be integrated into personal thermal monitoring systems or environmental warning systems to provide real-time assessment of thermal stress risk.

4.4. Limitations and future directions

The current model incorporates several simplifications that may affect predictive accuracy. The assumption of quasi-steady blood perfusion and metabolic heat generation may not fully capture dynamic cardiovascular responses to thermal stress. The model treats skin as a simplified layered structure without explicitly accounting for complex three-dimensional architecture of skin appendages, including hair follicles, sweat glands, and sebaceous glands, which can create preferential heat transfer pathways. In addition, evaporative cooling from sweating may further modulate skin temperature responses under sustained solar exposure.

Experimental validation was conducted under specific environmental conditions with limited subject population. Individual variations in skin thickness, pigmentation, age, and health status can significantly affect thermal responses and may require personalized model parameters. Environmental factors such as wind speed, humidity, and ambient temperature interact with solar radiation in complex ways that may not be fully captured by current boundary condition formulations.

Future research should focus on expanding the model to include additional physiological complexity, such as dynamic blood perfusion responses, sweat production effects, and clothing interactions. The development of personalized model parameters based on individual characteristics represents another important direction, where machine learning approaches could optimize DPL parameters for different population groups and environmental conditions.

5. Conclusions

In this study, a thermophysiological model incorporating the Dual Phase Lag (DPL) heat conduction theory was developed to investigate human thermal responses under dynamic solar radiation. The model's predictive performance was compared with that of the classical Pennes bioheat equation to validate its accuracy. Furthermore, the effects of solar radiation intensity and exposure duration on skin temperature were systematically analyzed. The main findings are summarized as follows:

(1) The DPL thermophysiological model enhanced accuracy in predicting skin temperature variations under dynamic solar radiation compared to the conventional Pennes model. This improvement highlights the importance of accounting for non-Fourier heat transfer behavior in transient thermal environments.

(2) With increasing exposure time, the rate of change in skin temperature approaches zero, indicating a tendency toward thermal equilibrium. Although the patterns of temperature rise and fall are similar in magnitude and shape, human thermal perception may differ due to the asymmetrical distribution of thermal receptors—specifically, the higher density of cold receptors makes individuals more sensitive to cooling than to heating.

(3) An obvious time lag was observed in the response of the inner skin layer. Over 15-minute intervals, the surface and inner skin temperatures often exhibited opposite trends. This depth-dependent temperature alternation—with surface temperatures showing more pronounced fluctuations than inner layers—suggests a complex interaction in thermal sensation mechanisms that cannot be captured by surface measurements alone.

(4) The amplitude of surface skin temperature fluctuations was positively correlated with solar radiation intensity. While the inner skin layer maintained good thermal stability under low radiation levels, exposure beyond a certain threshold disrupted this stability, indicating a nonlinear response to increasing thermal loads.

These findings provide some novel insights into the physiological mechanisms of human thermal perception under dynamic environmental conditions and offer a more accurate foundation for evaluating outdoor thermal comfort. The proposed DPL-based model can be further extended to explore heat stress and thermal comfort in broader environmental and occupational contexts.

CRediT authorship contribution statement

Yuchen Ji: Writing – original draft, Visualization, Software, Methodology, Investigation, Funding acquisition, Conceptualization. **Wei Gu:** Writing – review & editing, Visualization, Validation, Data curation. **Da Tao:** Writing – review & editing, Resources, Project administration, Formal analysis. **Pengyuan Shen:** Writing – review & editing, Writing – original draft, Supervision, Resources, Methodology, Conceptualization.

Declaration of competing interest

The authors declare that they have no known competing financial interests or personal relationships that could have appeared to influence the work reported in this paper.

Acknowledgement

The work presented in this paper was funded by the Foundation of Shenzhen Science and Technology Innovation Committee (Grant No. 20231122105927001).

Data availability

Data will be made available on request.

References

[1] Z. Ren, Y. Fu, Y. Dong, P. Zhang, X. He, Rapid urbanization and climate change significantly contribute to worsening urban human thermal comfort: A national 183-city, 26-year study in China, Urban Climate 43 (2022) 101154.
[2] P. Shen, Y. Li, X. Gao, S. Chen, X. Cui, Y. Zhang, X. Zheng, H. Tang, M. Wang, Climate Adaptability of Building Passive Strategies to Changing Future Urban Climate: A Review, Nexus 2 (2) (2025) 1–13.
[3] K. Li, Y. Zhang, L. Zhao, Outdoor thermal comfort and activities in the urban residential community in a humid subtropical area of China, Energ. Buildings 133 (2016) 498–511.
[4] Y. Peng, T. Feng, H. Timmermans, A path analysis of outdoor comfort in urban public spaces, Build. Environ. 148 (2019) 459–467.
[5] S. Thorsson, T. Honjo, F. Lindberg, I. Eliasson, E.-M. Lim, Thermal Comfort and Outdoor Activity in Japanese Urban Public Places, Environ. Behav. 39 (5) (2007) 660–684.
[6] S. Li, M. Wang, P. Shen, X. Cui, L. Bu, R. Wei, L. Zhang, C. Wu, Energy Saving and Thermal Comfort Performance of Passive Retrofitting Measures for Traditional Rammed Earth House in Lingnan, China, Buildings 12 (10) (2022) 1716.
[7] K. Blazejczyk, Influence of solar radiation on skin temperature in standing and walking subjects outdoors, S. Leszczycki Institute of Geography and Spatial Organization, Warszawa, Poland, 1999.
[8] K. Blazejczyk, H. Nilsson, I. Holmér, Solar heat load on man. Review of different methods of estimation, Int. J. Biometeorol. 37 (3) (1993) 125–132.
[9] M. Wang, P. Shen, Investigation of Indoor Asymmetric Thermal Radiation in Tibet Plateau: Case Study of a Typical Office Building, Buildings 12 (2) (2022) 129.
[10] F.R. de Gruijl, Skin cancer and solar UV radiation, Eur. J. Cancer 35 (14) (1999) 2003–2009.
[11] K. Danno, T. Horio, S. Imamura, Infrared radiation suppresses ultraviolet B-induced sunburn-cell formation, Arch. Dermatol. Res. 284 (2) (1992) 92–94.
[12] Y. Xiao, Y. Gao, Y. Wang, X. Meng, Effects of solar radiation on thermal sensation and physical fatigue of the human body under heavy-load exercise, Indoor Built Environ. 31 (1) (2022) 7–16.
[13] A.D. Seleznyov, S.K. Solanki, N.A. Krivova, Modelling solar irradiance variability on time scales from minutes to months, A&A 532 (2011) A108.
[14] Y. Ji, J. Song, P. Shen, A review of studies and modelling of solar radiation on human thermal comfort in outdoor environment, Build. Environ. 214 (2022) 108891.
[15] R.B. Roemer, J.R. Oleson, T.C. Cetas, Oscillatory temperature response to constant power applied to canine muscle, Am. J. Phys. Anthropol. 249 (2 Pt 2) (1985) R153–R158.
[16] A. Banerjee, A.A. Ogale, C. Das, K. Mitra, C. Subramanian, Temperature distribution in different materials due to short pulse laser irradiation, Heat Transfer Eng. 26 (8) (2005) 41–49.
[17] R.B. Chang, Body thermal responses and the vagus nerve, Neurosci. Lett. 698 (2019) 209–216.
[18] C. Liu, N. Zhang, Y. Li, X. Wang, J. Shi, W. Yao, W. Gao, A review of the application of EEG signals in the study of thermal comfort, J. Environ. Psychol. 103 (2025) 102580.
[19] M. Luo, F. Guo, H. Tang, R. Ming, L. Huang, H. Zhao, A systematic review of the influence of physiological factors on outdoor thermal comfort, Human Settlements and Sustainability 1 (1) (2025) 27–40.
[20] Y. Yang, J. Lyu, Z. Lian, Y. Xie, Y. Jiang, J. Lin, J. Niu, Subjective information in thermal comfort evaluation methods: A critical review, Energ. Buildings 325 (2024) 115019.
[21] A.P. Gagge, J.A.J. Stolwijk, Y. Nishi, An Effective Temperature Scale Based on a Simple Model of Human Physiological Regulatiry Response, Memoirs of the Faculty of Engineering, Hokkaido University 13 (Suppl) (1972) 21–36.
[22] S. Tanabe, K. Kobayashi, J. Nakano, Y. Ozeki, M. Konishi, Evaluation of thermal comfort using combined multi-node thermoregulation (65MN) and radiation models and computational fluid dynamics (CFD), Energ. Buildings 34 (6) (2002) 637–646.
[23] D. Fiala, G. Havenith, P. Brode, B. Kampmann, G. Jendritzky, UTCI-Fiala multi-node model of human heat transfer and temperature regulation, Int. J. Biometeorol. 56 (3) (2012) 429–441.
[24] K. Nagano, A. Takaki, M. Hirakawa, Y. Tochihara, Effects of ambient temperature steps on thermal comfort requirements, Int. J. Biometeorol. 50 (1) (2005) 33–39.
[25] J.B. Malchaire, Predicted sweat rate in fluctuating thermal conditions, Eur. J. Appl. Physiol. 63 (3) (1991) 282–287.
[26] Y. Zhang, J. Zhang, H. Chen, X. Du, Q. Meng, Effects of step changes of temperature and humidity on human responses of people in hot-humid area of China, Build. Environ. 80 (2014) 174–183.
[27] P.O. Fanger, Thermal comfort: analysis and applications in environmental engineering, McGraw-Hill, New York, 1972.
[28] R. de Dear, G. Brager, Developing an Adaptive Model of Thermal Comfort and Preference, ASHRAE Trans. 1041 (1998) 1–18.
[29] G.S. Brager, R.J. de Dear, Thermal adaptation in the built environment: a literature review, Energ. Buildings 27 (1) (1998) 83–96.
[30] P. Bröde, D. Fiala, K. Błażejczyk, I. Holmér, G. Jendritzky, B. Kampmann, B. Tinz, G. Havenith, Deriving the operational procedure for the Universal Thermal Climate Index (UTCI), Int. J. Biometeorol. 56 (3) (2012) 481–494.
[31] Y. Zhang, R. Zhao, Relationship between thermal sensation and comfort in non-uniform and dynamic environments, Build. Environ. 44 (7) (2009) 1386–1391.
[32] K.J.L. Dusan Fiala, M. Stohrer, First principles modeling of thermal sensation responses in steady-state and transient conditions, ASHRAE Trans. 109 (1) (2003) 179–186.
[33] J.W. Ring, R. de Dear, Temperature Transients: A Model for Heat Diffusion through the Skin, Thermoreceptor Response and Thermal Sensation, Indoor Air 1 (4) (1991) 448–456.
[34] W. Dong, D. Dai, P. Shen, R. Zhang, M. Liu, How Public Urban Space Enhance Restoration Benefits Through Combined Multisensory Effects: A Systematic Review, Land 13 (12) (2024) 2018.
[35] W. Dong, D. Dai, M. Liu, Y. Wang, S. Li, P. Shen, Combined effects of the visual-thermal environment on restorative benefits in hot outdoor public spaces: A case study in Shenzhen, China, Building and Environment 272 (2025) 112690.
[36] K. Lindner-Cendrowska, K. Błażejczyk, Impact of selected personal factors on seasonal variability of recreationist weather perceptions and preferences in Warsaw (Poland), Int. J. Biometeorol. 62 (1) (2018) 113–125.
[37] H.F. Blum, The Physiological Effects of Sunlight on Man, Physiol. Rev. 25 (3) (1945) 483–530.
[38] W.L. Roller, R.F. Goldman, Estimation of solar radiation environment, Int. J. Biometeorol. 11 (3) (1967) 329–336.
[39] W.L. Roller, R.F. Goldman, Prediction of solar heat load on man, J. Appl. Physiol. 24 (5) (1968) 717–721.
[40] Z. Wang, H. Yu, M.H. Luo, Z. Wang, H. Zhang, Y. Jiao, Predicting older people's thermal sensation in building environment through a machine learning approach: Modelling, interpretation, and application, Build. Environ. 161 (2019).
[41] Y.X. Xie, J.L. Niu, H. Zhang, S.J. Liu, J.L. Liu, T.Y. Huang, J.N. Li, C.M. Mak, Development of a multi-nodal thermal regulation and comfort model for the outdoor environment assessment, Build. Environ. 176 (2020).
[42] X. Zhou, H. Zhang, Z.W. Lian, Y.F. Zhang, A model for predicting thermal sensation of Chinese people, Build. Environ. 82 (2014) 237–246.
[43] S. Hodder, K. Parsons, The effects of solar radiation and black body re-radiation on thermal comfort, Ergonomics 51 (4) (2008) 476–491.
[44] M.Y. Akhalaya, G.V. Maksimov, A.B. Rubin, J. Lademann, M.E. Darvin, Molecular action mechanisms of solar infrared radiation and heat on human skin, Ageing Res. Rev. 16 (2014) 1–11.
[45] S. Chaiyapinunt, N. Khamporn, Effect of solar radiation on human thermal comfort in a tropical climate, Indoor Built Environ. 30 (3) (2021) 391–410.
[46] X. Xiang, Y. He, N. Li, Evaluating annual thermal discomfort time ratio of indoor occupants caused by solar radiation using a novel model, Architectural Intelligence 3 (1) (2024) 26.
[47] S.G. Hodder, K. Parsons, The effects of solar radiation on thermal comfort, Int. J. Biometeorol. 51 (3) (2007) 233–250.
[48] B.R. Kingma, A.J. Frijns, L. Schellen, W.d., van Marken Lichtenbelt, Beyond the classic thermoneutral zone: Including thermal comfort, Temperature (Austin) 1 (2) (2014) 142–149.
[49] I. Kohri, T. Mochida, Evaluation Method of Thermal Comfort in a Vehicle with a Dispersed Two-Node Model.br.Part 1—Development of Dispersed Two-Node Model, Journal of the Human-Environment, System 6 (1) (2002) 19–29.
[50] E. Foda, K. Siren, A new approach using the Pierce two-node model for different body parts, Int. J. Biometeorol. 55 (4) (2011) 519–532.
[51] S. Takada, H. Kobayashi, T. Matsushita, Thermal model of human body fitted with individual characteristics of body temperature regulation, Build. Environ. 44 (3) (2009) 463–470.
[52] O. Kaynakli, U. Unver, M. Kilic, Evaluating thermal environments for sitting and standing posture, Int. Commun. Heat Mass Transfer 30 (8) (2003) 1179–1188.
[53] O. Kaynakli, M. Kilic, Investigation of indoor thermal comfort under transient conditions, Build. Environ. 40 (2) (2005) 165–174.
[54] K. Katić, R. Li, W. Zeiler, Thermophysiological models and their applications: A review, Build. Environ. 106 (2016) 286–300.
[55] A. Zolfaghari, M. Maerefat, A new simplified thermoregulatory bioheat model for evaluating thermal response of the human body to transient environments, Build. Environ. 45 (10) (2010) 2068–2076.
[56] H.H. Pennes, Analysis of Tissue and Arterial Blood Temperatures in the Resting Human Forearm, J. Appl. Physiol. 1 (2) (1948) 93–122.
[57] M. La Gennusa, A. Nucara, G. Rizzo, G. Scaccianoce, The calculation of the mean radiant temperature of a subject exposed to the solar radiation—a generalised algorithm, Build. Environ. 40 (3) (2005) 367–375.
[58] C. Marino, P. Misiani, A. Nucara, M. Pietrafesa, The effect of the climatic condition on the radiant asymmetry, Int. J. Heat Technol. 35 (Special Issue1) (2017) S419–S426.
[59] E. Arens, T. Hoyt, X. Zhou, L. Huang, H. Zhang, S. Schiavon, Modeling the comfort effects of short-wave solar radiation indoors, Build. Environ. 88 (2015) 3–9.
[60] K. Blazejczyk, G. Havenith, R. Szymczak, Simulations of the human heat balance during Mount Everest summit attempts in spring and winter, Int. J. Biometeorol. 68 (2023) 3.
[61] C. Huizenga, Z. Hui, E. Arens, A model of human physiology and comfort for assessing complex thermal environments, Build. Environ. 36 (6) (2001) 691–699.
[62] W. Kaminski, Hyperbolic Heat Conduction Equation for Materials With a Nonhomogeneous Inner Structure, Asme J Heat Transfer 112 (3) (1990) 555–560.
[63] Y. Gilaberte, L. Prieto-Torres, I. Pastushenko, Á. Juarranz, Chapter 1 - Anatomy and Function of the Skin, in: M.R. Hamblin, P. Avci, T.W. Prow (Eds.), Nanoscience in Dermatology, Academic Press, Boston, 2016, pp. 1–14.
[64] K. Mitra, S. Kumar, A. Vedevarz, M.K. Moallemi, Experimental Evidence of Hyperbolic Heat Conduction in Processed Meat, Journal of Heat Transfer 117(3) (1995) 568-573.
[65] D.Y. Tzou, Experimental support for the lagging behavior in heat propagation, J. Thermophys Heat Transfer 9 (4) (1995) 686–693.
[66] E.A.N. Al-Lehaibi, H.M. Youssef, The heat transfer in skin tissues under the general two-temperature three-phase-lag model of heat conduction with a comparative study, Heliyon 10 (22) (2024).

[67] P. Udayraj, R. Talukdar, A. Alagirusamy, Das, Heat transfer analysis and second degree burn prediction in human skin exposed to flame and radiant heat using dual phase lag phenomenon, Int. J. Heat Mass Transf. 78 (2014) 1068–1079.

[68] L. Vanggaard, K. Kuklane, A. Halder, The "AVA - organ", Extrem Physiol Med 4 (Suppl 1) (2015) A95.

[69] A. Nakayama, F. Kuwahara, A general bioheat transfer model based on the theory of porous media, Int. J. Heat Mass Transf. 51 (11) (2008) 3190–3199.

[70] M.J. Caterina, M.A. Schumacher, M. Tominaga, T.A. Rosen, J.D. Levine, D. Julius, The capsaicin receptor: a heat-activated ion channel in the pain pathway, Nature 389 (6653) (1997) 816–824.

[71] M.J. Caterina, A. Leffler, A.B. Malmberg, W.J. Martin, J. Trafton, K.R. Petersen-Zeitz, M. Koltzenburg, A.I. Basbaum, D. Julius, Impaired nociception and pain sensation in mice lacking the capsaicin receptor, Science 288 (5464) (2000) 306–313.

[72] Chapter 3 - Absorption and Scattering of Solar Radiation in the Atmosphere, in: K. N. Liou (Ed.), International Geophysics, Academic Press2002, pp. 65-115.

[73] Z.-S. Deng, J. Liu, Parametric studies on the phase shift method to measure the blood perfusion of biological bodies, Med. Eng. Phys. 22 (10) (2000) 693–702.

[74] P. Kumar, D. Kumar, K.N. Rai, Numerical simulation of dual-phase-lag bioheat transfer model during thermal therapy, Math. Biosci. 281 (2016) 82–91.

[75] D. Kumar, P. Kumar, K.N. Rai, Numerical solution of non-linear dual-phase-lag bioheat transfer equation within skin tissues, Math. Biosci. 293 (2017) 56–63.

[76] G.D. Smith, Numerical Solution of Partial Differential Equations: Finite Difference Methods, Clarendon Press, 1985.

[77] Y. Ji, J. Song, P. Shen, A data-driven model on human thermophysiological and psychological responses under dynamic solar radiation, Build. Environ. 248 (2024) 111098.

[78] S. Hodder, B. Palella, Measurement and Quantification of Thermal Environments; ISO 7726 -Ergonomics of the Thermal Environment - Instruments and methods for measuring and monitoring physical quantities, 6 (2024) 18-22.

[79] D. Analog, DS1923: iButton Hygrochron Temperature/Humidity Logger with 8KB Data-Log Memory Data Sheet, Analog Devices Rev. 9 (2009).

[80] H. Askarizadeh, H. Ahmadikia, Analytical analysis of the dual-phase-lag model of bioheat transfer equation during transient heating of skin tissue, Heat Mass Transf. 50 (12) (2014) 1673–1684.

[81] P.J. Rodríguez de Rivera, M. Rodríguez de Rivera, F. Socorro, M. Rodríguez de Rivera, Experimental study of the thermal probing depth of a skin calorimeter, Int. J. Heat Mass Transf. 212 (2023) 124258.

[82] S. Nie, C. Zhang, J. Song, Thermal management of epidermal electronic devices/ skin system considering insensible sweating, Sci. Rep. 8 (1) (2018) 14121.

[83] M. Igaki, T. Higashi, S. Hamamoto, S. Kodama, S. Naito, S. Tokuhara, A study of the behavior and mechanism of thermal conduction in the skin under moist and dry heat conditions, Skin Res. Technol. 20 (1) (2014) 43–49.

[84] D.Y. Tzou, A Unified Field Approach for Heat Conduction From Macro- to Micro-Scales, J. Heat Transfer 117 (1995).

[85] M. Wang, N. Yang, Z.-Y. Guo, Non-Fourier heat conductions in nanomaterials, J. Appl. Phys. 110 (6) (2011).

[86] A. Banerjee, O.A. A., D. Champak, M. Kunal, C. and Subramanian, Temperature Distribution in Different Materials Due to Short Pulse Laser Irradiation, Heat Transfer Engineering 26(8) (2005) 41-49.